Dynamics of binary liquids in pores

J. C. Lee
Physics Department and Program in Scientific Computing, University of Southern Mississippi, Hattiesburg, Mississippi 39406-5046
(Received 7 August 1995)

A computer simulation is performed to study the dynamics of binary liquids in the pores of Vycor glasses. The pores are modeled with glass walls that form randomly interconnected tunnels. When the relaxation is probed with a particular wavelength, the time autocorrelation function depends on whether or not there is a significant periodic or quasiperiodic structure in the distribution of the walls with that wavelength. If there is not, the relaxation may be fitted as the sum of an exponential term and a nonexponential activated term. If there is, the relaxation shows a long-lasting tail that can be fitted by introducing an additional constant term in the above fitting function. The relaxation time measured from the exponential term supports the dynamic scaling with the same dynamic exponent as in the bulk. In the long length scales, however, the data show a trend of deviation from this scaling in the direction of faster relaxation. We interpret this behavior as a confining effect of the walls.

PACS number(s): 68.45.Gd, 05.40.+j, 64.60.Ht, 05.50.+q

I. INTRODUCTION

When binary liquid mixtures are embedded in the pores of Vycor glass [1–5], the glass walls affect the equilibrium dynamics of the liquid mixture in a profound way, which is not yet fully understood. If the pore size is much shorter than the correlation length, the effect is well explained with a random-field model. Dierker and Wiltzius (DW) [2] performed a dynamic light scattering experiment using samples of lutidine-water mixtures embedded in the pores of a Vycor glass of pore size 30 Å. The results for the time autocorrelation function may be fitted remarkably well as the sum of an exponential diffusive term and a nonexponential activated term. The activation term is given by $\exp(-x^3)$, where $x=\ln(t/\tau_0)/\ln(\tau/\tau_0)$ demonstrates the activated dynamic scaling that Huse [6] predicted for random field Ising models with a conserved order parameter. Here τ_0 is the smallest time scale.

Aliev, Goldburg, and Wu (AGW) [5] explored the opposite regime, where the pore size is much larger than the correlation length, using samples of carbon disulfate–nitromethane mixture embedded in the pores of a macroporous glass with pore size as large as 1000 Å. The results for the autocorrelation function show different patterns of relaxation depending on whether the samples are isolated or kept in contact with a reservoir. When the samples are isolated as in the experiment by DW, although the pores should be large enough for the mixtures to behave as in the bulk, the relaxation is not exponential; the data can only be fitted with $1/(1+x^3)$. While this is a very slow function, the relaxation time entering in x is shorter than the relaxation time in the bulk. When the scattering angle is small, this phenomenon is even more pronounced and the usual q^2 dependence of the relaxation rate on the wave vector breaks down. AGW explain this anomalous q dependence in terms of a Brownian particle that diffuses in a much restricted one-dimensional box. These cannot be regarded as a result of random fields.

Liu *et al.* [7] argued that much of the random-field-like behavior, such as metastability, may also be explained as a wetting effect in a confined geometry and introduced a single pore model. But the time autocorrelation function has not yet been computed with any model of glass pores. The purpose of this paper is to compute the time autocorrelation function treating the effects of the glass walls in far more detail than is implicit in the random-field models. The model is constructed in Sec. II. The results for the time autocorrelation function are presented in Sec. III. The pattern of relaxation is the same as that found by DW. In Sec. IV we show that the results for the relaxation time in the exponential term exhibit a limited form of scaling behavior, but with a notable pattern of deviation when the scaling variable involves small wave vectors. This is interpreted as a confining effect of the glass walls.

II. MODEL

The pores of Vycor glass look like interconnected tunnels. The structure is random in the sense that the tunnels wind, split into two, etc., all in an unpredictable fashion, but the tunnel size is distributed rather sharply [8,9]. Thus we model the glass pores with randomly interconnected tunnels of fixed width. On a square lattice of 256×256, $\frac{256}{8}=32$ equally spaced horizontal rows are chosen. Along each of these rows, draw straight lines, 16 lattice spacings long, with random gaps, varying in length between 1 and 12 lattice spacings. To maintain the periodic boundary condition, one line or more on each row may be less than 16. All the lattice sites on these lines are to be occupied by impurity atoms, which make disconnected walls.

Two comments are in order concerning this model for the walls of the glass. First, the disconnected walls create many loosely interconnected tunnels. By tunnels we mean narrow regions bound by two walls, one above and

one below, with openings at the left and right ends. In this regard, the model may be regarded as a multi-pore extension of the single-pore model of Liu *et al.* [7]. Second, the model is unrealistic in many ways; the walls are all thin, straight, disconnected, and on horizontal rows. It is easy to generate more realistic models by performing a spinodal decomposition [9,10], but instead we wish to address a more difficult problem with a simpler model. Frisken, Ferri, and Cannell [11] and Lin *et al.* [4] emphasized the importance of the adsorption clusters (layers) in static behavior. These clusters are expected to relax very slowly, if at all. With the thin and straight walls distributed as in the model, we have forced this effect to occur in only a certain number of wave vectors. The contrast in the relaxation pattern in these wave vectors and elsewhere will provide us with useful information about the role of the adsorption clusters in dynamics.

Consider now a binary mixture of A and B represented by ferromagnetic Ising spins. The spins occupy all lattice sites except the sites on the walls. The impurity atoms in the walls remain frozen and impose a field (chemical potential) on their neighboring spins so as to favor one component, say, the minus spins, in their vicinity and effectively to push the plus spins away from them. The Hamiltonian is given by

$$H=-J\sum_{\langle i,j\rangle}S_iS_j+\sum_i h_iS_i\ , \tag{1}$$

where $S_i=+1$ (A atoms), $S_i=-1$ (B atoms), $S_i=0$ (wall atoms), and the symbol $\langle ij\rangle$ limits the sum to nearest-neighbor pairs of spins. The field in the second term is given by $h_i=hn_i$, where h is a constant and n_i is one if spin i is adjacent to a wall and zero otherwise. The time evolution is governed by the Kawasaki spin exchange dynamics, which allows only exchanges of nearest-neighbor pairs of opposite spins, thus conserving the order parameter.

The composition ratio $A:B$ is 50:50 and $h=0.8$ (with J and the Boltzmann constant set to unity). We will investigate the equilibrium dynamic behavior in the one-phase region at $T=1.5T_C$, $1.1T_C$, and $1.05T_C$, where T_C is the transition temperature of the pure two-dimensional Ising model.

III. COMPUTATIONS AND RESULTS

We measure the equal-time static structure factor

$$S(q)=\langle\rho(q)\rho(-q)\rangle \tag{2}$$

and the equilibrium time-autocorrelation function

$$g(q,t)=\langle\rho(q,t+t_0)\rho(-q,t_0)/S(q)\rangle\ , \tag{3}$$

where $\rho(q,t)=\sum\exp(iqr_i)S_i$ is the concentration fluctuation and the ensemble average includes the average over different initial times denoted by t_0. The time will be given in units of Monte Carlo steps (MCS). In one MCS, each nearest-neighbor pair is chosen once on average and an exchange is attempted. For each temperature, we thermalize the spin configuration for a long time until the equal-time structure factor shows no persistent pattern of change, which we take as a sign of an equilibrium or quasiequilibrium state. For $T=1.1T_C$ and $1.05T_C$, this process of thermalization takes more time than the actual measurements. Once the thermalization is completed, we take the last configuration as the initial configuration [see Eq. (3)] and compute the autocorrelation at the delay times t given by $t_1=1$, $t_2=2t_1$, $t_3=2t_2$, ..., and $t_{11}=1024$ MCS. This is repeated approximately 1500 times always taking the last configuration of the preceding measuring period as the initial configuration. Taking the average over these 1500 measurements, we obtain the final results for each delay time. For each temperature this takes approximately 1.536×10^6 MCS.

First, we compute the glass structure factor with the result shown in Fig. 1(b). The wave vector q is given in units of $2\pi/L$, where $L=256$. The corresponding wavelength is $\lambda=L/q$. There are two prominent peaks at $q=32$ and 64 and two faint peaks at $q=13$ and 22. The two strong peaks at $q=32$ and 64 are the Bragg peaks resulting from the regular placement of the rows of walls eight lattice spacings apart along the vertical direction. The two faint peaks come from the quasiregular wall structure along the horizontal direction; the peak at $q=22$ corresponds to the average wall length and the peak at $q=13$ corresponds to the average length of the quasibasic units in each row of walls, namely, a wall and a gap. The structure factor hardly falls off starting from

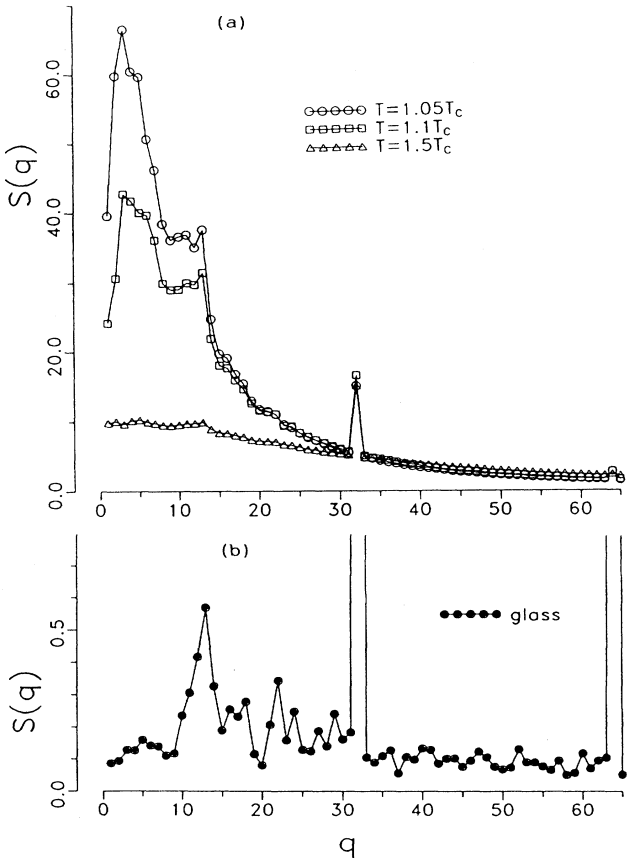

FIG. 1. (a) Spin structure factors (arbitrary units). (b) Glass structure factor (arbitrary units). The wave vector q is given in units of $2\pi/L$, where $L=256$ lattice spacings.

about $q=35$, which is due to the small walls and gaps in the small length scales.

As Fig. 1(a) shows, the four peaks of the glass structure factor reappear in the spin structure factor. This suggests that the composition fluctuations along the horizontal direction have the same pattern as the wall structure. This is because adsorption clusters of species B coat the walls. The presence of such adsorption clusters (layers) was observed in two previous experiments [4,9].

Figure 2 shows $g(q,t)$ as a function of q after the longest delay time t_{11} that we have measured. We find here again the q-dependent signature of the wall structure. The two peaks at $q=13$ and 22 are now quite noticeable, suggesting that the adsorption clusters relax very slowly. Thus the walls have divided the atoms into two dynamic groups: the semifrozen atoms in the adsorption clusters and the free atoms elsewhere, as observed by Frisken and Cannell [12] for binary liquids in gel.

In Fig. 3 we attempt to fit the same data as a function of time in the form of

$$g(q,t)=A_D\exp(-t/\tau_D) + A_A\exp\{-[\ln(t)/\ln(\tau_A)]^2\}\ , \quad (4)$$

where the first exponential term represents the fast modes of relaxation due to the free atoms and the second nonexponential term the slow modes [6] due to the semifrozen atoms. This works quite well in the regime of small q, i.e., when the system is probed with a wavelength larger than the length scales of the periodic or quasiperiodic structures of the walls. The fitting turns out to be reasonably good for $q=13$ and 22 also, but this is presumably because the delay time was not extended long enough. It definitely does not work when the wavelength matches the periodicity of the walls along the vertical direction or the quasiperiodicity along the horizontal direction. The former is the case at $q=32$, 64, ... and the latter approximately at all $q>40$. In these cases, $g(q,t)$ exhibits a long-lasting tail that cannot be fit with Eq. (4). If we assume that the tail has a nonvanishing asymptotic limit, then the data can be fit by introducing an additional parameter C to Eq. (4). Since the data are taken at finite times, this does not necessarily mean that $g(q,t=\infty)$ is finite; it only means that the relaxation slows down as if it were approaching a finite asymptotic limit. Figures 4–7 show the results for the fitting parameters. The results

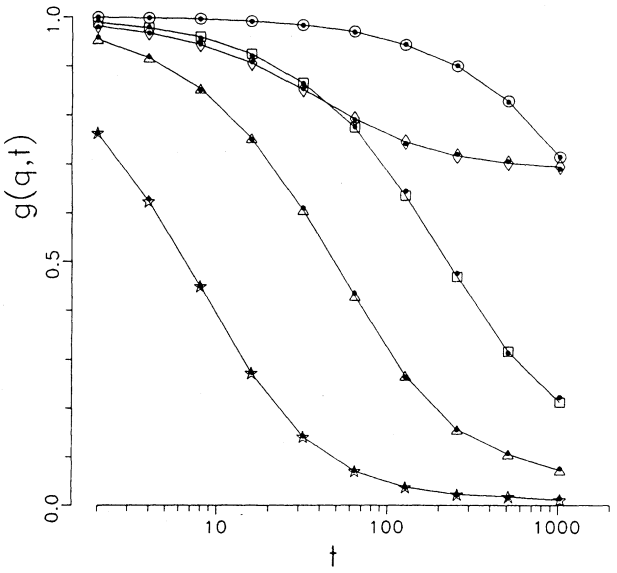

FIG. 3. Time autocorrelation function as a function of delay time t (in units of MCS) at $T=1.1T_C$; the large open symbols represent the computed data points and the small filled circles the best fit; the lines connect the computed data points. The symbols represent $q=10$ (circles), $q=32$ (diamonds), $q=20$ (squares), $q=30$ (triangles), and $q=40$ (stars).

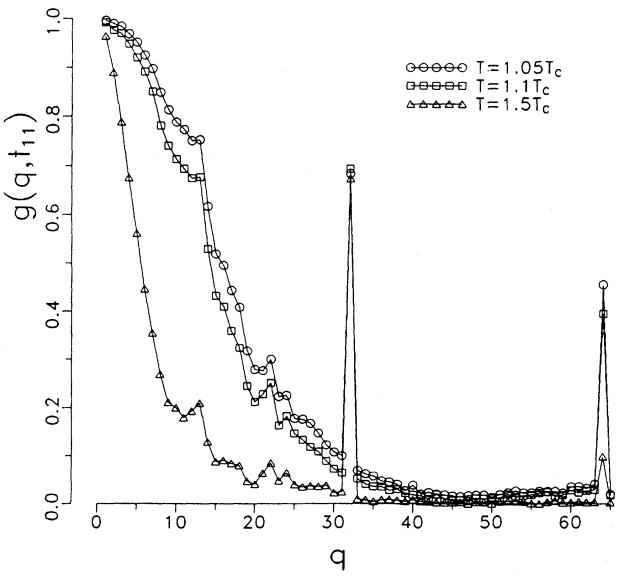

FIG. 2. Time autocorrelation function (unitless) as a function of q after the longest delay time $t_{11}=1024$ MCS.

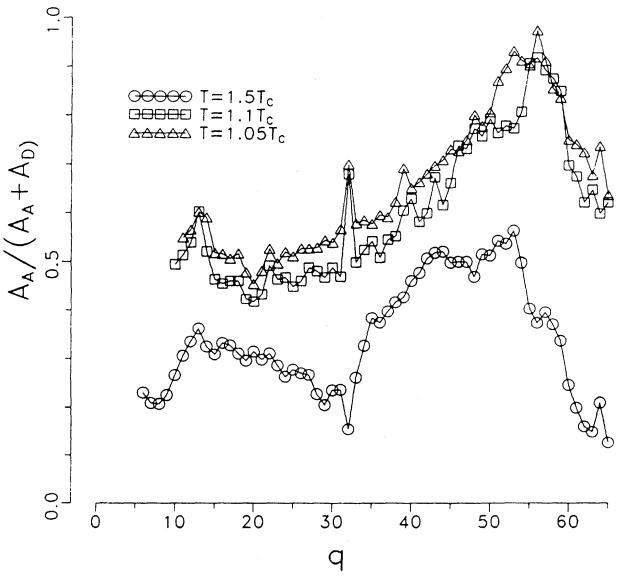

FIG. 4. Ratio of the activated amplitude versus the activated amplitude plus the nonactivated amplitude.

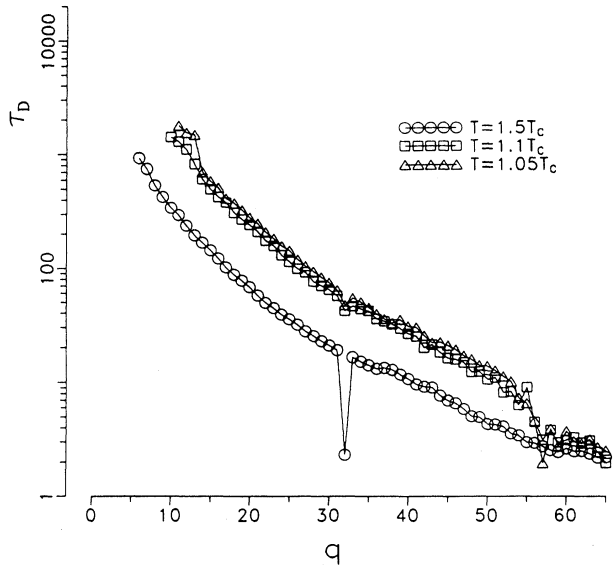

FIG. 5. Nonactivated relaxation time.

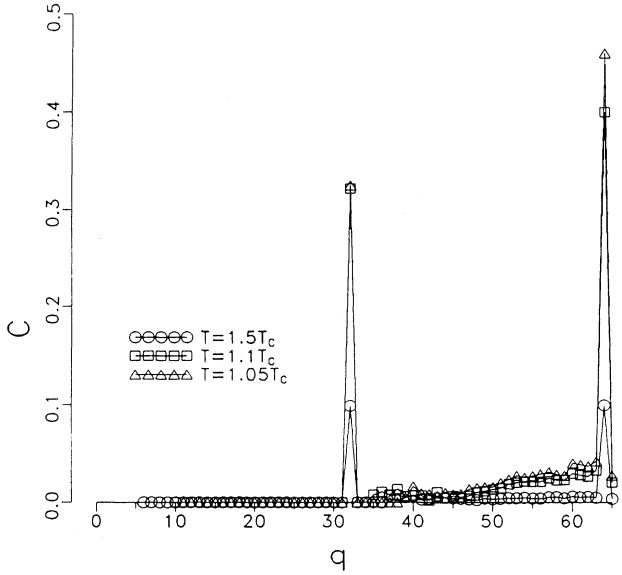

FIG. 7. "Nonrelaxing" constant term.

for $A_A/(A_A+A_D)$ and τ_A show that the activation term becomes more and more important as q increases and also as T decreases. The results for C show a pattern similar to $g(q,t_{11})$, as expected.

It is difficult to determine the fitting parameters accurately because with χ^2 alone one cannot distinguish different combinations of A_A and A_D very sharply nor, for a given A_A, different combinations of τ_A and C. Rather surprisingly, τ_D is quite different in this regard. The results for τ_D are less sensitive to the choice of these combinations and prove more reliable, except at very small q and very large q. This is because at very small q there is not much relaxation even when the delay time t reaches t_{11}. (The case of $T=1.5T_C$ is an exception. Here the relaxation is fast enough to allow the data to be fitted down to $q=1$.) At large q, on the other hand, the relaxation is very fast and the data cannot reflect the effects of the exponential term adequately; by the time t reaches t_1, a considerable amount of relaxation has already occurred. We will analyze the results for τ_D further in Sec. IV.

Figure 8 shows a typical morphology at $T=1.05T_C$. The adsorption clusters clogging up the tunnels are quite noticeable; such overgrown adsorption clusters will be called plugs, following Liu *et al.* [7]. There is also a small number of tunnels with adsorption clusters anchored to one single wall, thus allowing some nonpreferred atoms

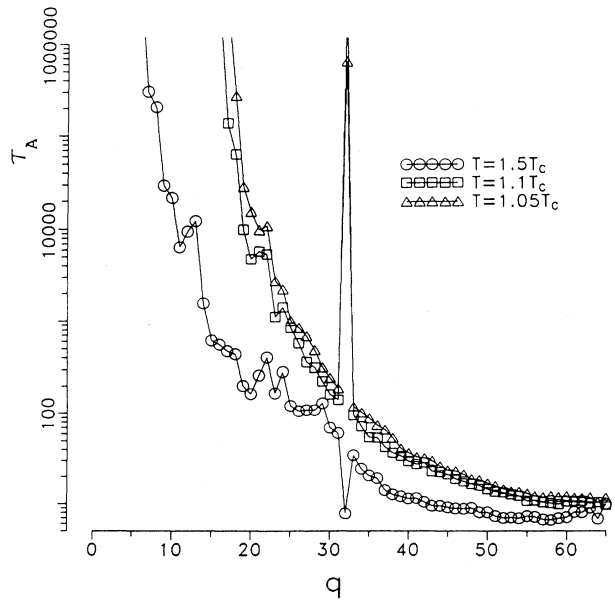

FIG. 6. Activated relaxation time.

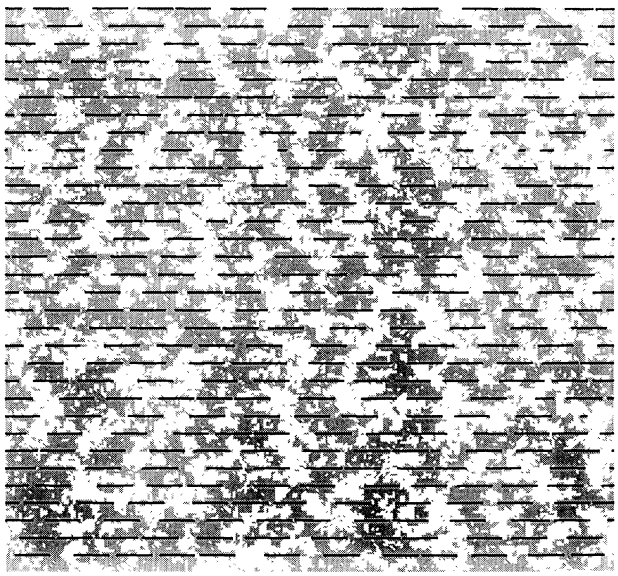

FIG. 8. Typical morphology at $T=1.05T_C$. The large black dots represent the wall atoms, the gray shade the preferred atoms, and the blanks the nonpreferred atoms.

in the tunnel. In such tunnels a plug is either in the process of being formed or in the process of being broken up. The fact that such tunnels constitute only a small fraction of the total indicates that the plugs remain, once formed, for a long time, which is the cause of the activated relaxation. Figure 9 shows the morphology at $T=1.5T_C$. The plugs are now quite unstable and have turned into less dominant adsorption clusters of very ragged shape. Although the dynamics is faster than at $T=1.05T_C$, the presence of the walls still leads to an activated relaxation. It should be mentioned here that the dynamics of the pure Ising model itself is activated not only at $T=0$ [13] but also at $T>T_C$ [14]. In the presence of the field term, we find that this remains the case by a significant margin. For example, at $T=1.5T_C$ and $q=10$, the activated relaxation time is longer than in the pure system by an order of magnitude.

In the pure system, the relaxation time τ is a homogeneous function of the wave vector q and the correlation length ξ. This results in two expressions of dynamic scaling [15]

$$\tau(q,T)\xi^{-z}=f(q\xi) \tag{5}$$

and

$$\tau(q,T)q^{z}=h(q\xi)\ , \tag{6}$$

where z is the dynamic exponent. We wish to find out whether or not the results for τ_D support these scaling laws, assuming $z=4-\eta=3.75$ as in the pure system. For comparison, we repeat the same computations for the pure system without the walls. The results are shown in Fig. 10. The scaling holds approximately in both cases. But when the walls are present there is a noticeable sign of deviation for small q; the lone circle far away from the rest corresponds to $q=32$. In fact, the results for τ_D are approximately the same as in the pure system except in long length scales (small q). Let us examine the scaling function. Taking the data for $T=1.1T_C$, which appear in the middle portion of the exhibited data, the best fit gives $f(x)\sim x^{-3.0\pm0.2}$ and $h(x)\sim x^{0.8\pm0.2}$. This is consistent with the assumed value of z, since the two scaling laws imply $f(x)=x^{-z}h(x)$, which is approximately satisfied. Here the system is in the critical regime, but not at the critical limit, where $f(x)$ should behave like x^{-z}. In the hydrodynamic regime of small x and small q, on the other hand, $f(x)\sim x^{-1.8\pm0.2}$. This could be interpreted either as the same deviation from the scaling when q is small or as being consistent with the correct scaling function x^{-2}.

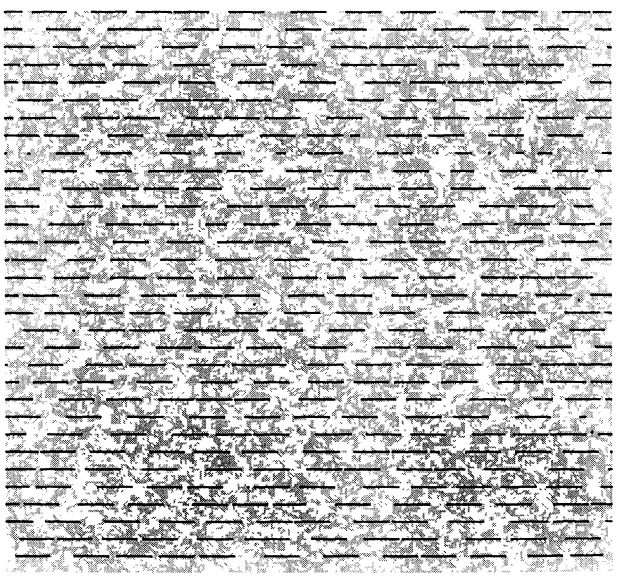

FIG. 9. Typical morphology at $T=1.5T_C$.

IV. DISCUSSION

Why does the scaling fail when the relaxation is probed for long length scales? We attempt to explain this in the following way. In the presence of the walls, the atoms lose a great number of paths that connects two lattice sites. A tagged free atom cannot go *through* the walls; it can only go *around*. Thus the pertinent distance is the

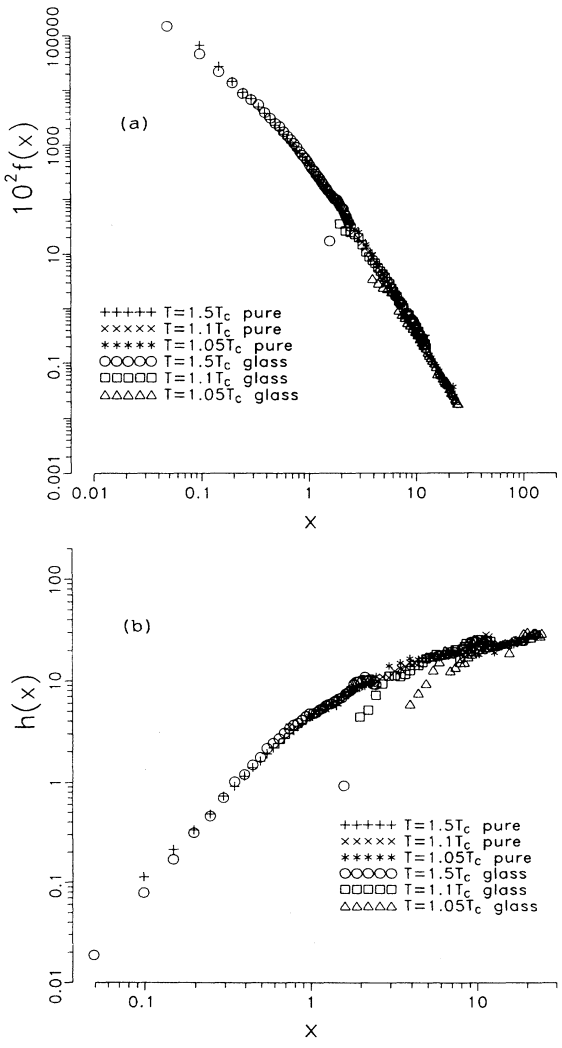

FIG. 10. Scaling plots for systems with and without the walls using (a) Eq. (5) and (b) Eq. (6).

minimum distance (also called cow distance, taxi distance, or chemical distance) [16], which goes around the walls, rather than the Pythagorean distance, which goes through the walls. With this in mind, take a lattice site and consider all the other sites at the Pythagorean distance of, say, l. What if the distance is now measured along the minimum path? If l is very small, the chance of finding the minimum distance different from l is relatively small. If l is large, on the other hand, the probability is overwhelmingly large. We believe that this is the reason for the deviation from the scaling when the scaling variable x involves small q. It has been shown that the walls have a similar effect in the nonequilibrium domain-growth kinetics. When a binary system is quenched from the infinite temperature into the unstable part of the two-phase region, phase-separated domains begin to grow. If the domain size is measured in the Phythagorean distance, its growth kinetics shows no sign of scaling [10], but if it is measured in the minimum distance the growth kinetic does exhibit a scaling behavior [17].

As mentioned earlier, our data are not accurate enough to determine whether or not this deviating trend from the scaling also extends to the hydrodynamic regime where x and q are both small. We see no compelling reason why the trend should stop in this regime and therefore we assume that the scaling breaks down in the hydrodynamic regime as well. If so, it means that the relaxation rate does not depend on q like $\Gamma \sim q^2$ anymore. We attempt to explain this in the following way. Since the free atoms can only diffuse in a highly constricted space between the adsorption clusters, the diffusion equation is different from place to place depending on the shape of the space available for the free atoms. Suppose that the space is wide open at certain parts (to be called region 1) while it is so narrowly constructed in some other parts (to be called regions 2 and 3) that the space is no more than a one-dimensional channel. The free atoms can diffuse in any direction in region 1, but only in the horizontal direction in region 2 and in the vertical direction in region 3. Now tag a free atom and consider its random motion in such a confined space. The probability density that it will have changed its position by $\mathbf{r}$ after time t is given by

$$\partial P(\mathbf{r},t)/\partial t = D\Delta(\mathbf{r})P(\mathbf{r},t) , \tag{7}$$

where D is the diffusion coefficient and $\Delta(\mathbf{r})$ is different depending on $\mathbf{r}$; it is $\partial^2/\partial x^2+\partial^2/\partial y^2$ in region 1, $\partial^2/\partial x^2$ in region 2, and $\partial^2/\partial y^2$ in region 3. As a result, the Fourier transform of $P(\mathbf{r},t)$ is poorly defined. Substituting $P(\mathbf{r},t)=(2\pi)^{-2}\int d^2q\, P(\mathbf{q},t)\exp(i\mathbf{q}\cdot\mathbf{r})$ in Eq. (7), we find

$$\partial P(\mathbf{q},t)/\partial t = -D\zeta(\mathbf{q})P(\mathbf{q},t) , \tag{8}$$

where, for a given $\mathbf{q}=(q_x,q_y)$, $\zeta(\mathbf{q})=\zeta_1=q_x^2+q_y^2$ in region 1, $\zeta=\zeta_2=q_x^2$ in region 2, and $\zeta=\zeta_3=q_y^2$ in region 3. Taking an average of Eq. (8) over different regions, we may write approximately for an $\mathbf{r}$-independent $P(\mathbf{q},t)$ in the form

$$\partial P(\mathbf{q},t)/\partial t = -D\zeta'(\mathbf{q})P(\mathbf{q},t) , \tag{9}$$

where $\zeta'(\mathbf{q})=c_1\zeta_1+c_2\zeta_2+c_3\zeta_3\sim q^v$, with $c_1+c_2+c_3=1$ and $v<2$. This may be the reason why the deviation from the scaling is in the direction of reducing the exponent below 2.

To compare the results of the present model with the experimental results of DW and AGW, note that with $\nu=1$, $\xi\approx(1-T/T_C)^{-\nu}$ is two lattice spacings at $T=1.5T_C$ and 20 lattice spacings at $T=1.05T_C$. Thus the system is closer to the samples used by DW at $T=1.05T_C$ and to the samples used by AGW at $T=1.5T_C$. Our results for the autocorrelation function are in qualitative agreement with DW but not with AGW. Surprisingly, however, the phenomenon of accelerated relaxation when q is small is in a qualitative agreement with AGW. Perhaps this should not be regarded as a surprise since the walls should have the aforementioned confining effect regardless of the pore size. The same effect has also been observed in a recent study on a gel model [18]. Work is in progress with a more realistic glass model, which should be closer to the samples used by AGW than the present model is.

Now we compare the present model with the random-field Ising models [19]. In the latter, rare statistical fluctuations leave regions of aligned fields here and there in a lumpy fashion. The aligned fields result in aligned spins, which may be regarded as the random-field analog of the adsorption clusters. In the present model, on the other hand, there are aligned fields next to all walls, which result in the same type of activated relaxation. But the adsorption clusters are much larger and more extended than in the random-field models, which has two important consequences. First, since they occupy so much space, it is meaningless to compare the correlation length and the pore size; even if the pore size is larger than the correlation length, the free atoms presumably do not actually have enough space to behave like in the bulk. Second, the adsorption clusters are large enough to break down the scaling behavior of the pure system in long length scales. In the random-field models, the details of the walls are ignored, which one may expect to be justified if the system is probed in long length scales. This is not the case, which is quite ironic.

ACKNOWLEDGMENTS

The computation was performed on a Cray-YMP at the Mississippi Center for Supercomputing Research. This research was supported by Donors of the Petroleum Research Funds administered by the American Chemical Society.

[1] M. C. Goh, W. I. Goldburg, and C. M. Knobler, Phys. Rev. Lett. **58**, 1088 (1987).
[2] S. B. Dierker and P. Wiltzius, Phys. Rev. Lett. **58**, 1865 (1987).
[3] P. W. Wiltzius, S. B. Dierker, and B. S. Dennis, Phys. Rev. Lett. **62**, 804 (1989); S. B. Dierker and P. Wiltzius, *ibid.* **66**, 1185 (1991).
[4] M. Y. Lin, S. K. Sinha, J. M. Drake X.-l. Wu. P. Thiyagarajan, and H. B. Stanley, Phys. Rev. Lett. **72**, 2207 (1994).
[5] F. Aliev, W. I. Goldburg, and X.-l. Wu, Phys. Rev. E **47**, R3834 (1993).
[6] D. A. Huse, Phys. Rev. B **36**, 5383 (1987).
[7] A. J. Liu, D. J. Durian, E. Herbolzheimer, and S. A. Safran, Phys. Rev. Lett. **65**, 1897 (1990); L. Monette, A. J. Liu, and G. S. Grest, Phys. Rev. A **46**, 7664 (1992); A. J. Liu and G. S. Grest, *ibid.* **44**, R7894 (1991).
[8] P. Levitz and D. Tchoubar, J. Phys. (France) I **2**, 771 (1992).
[9] L. Monette, G. S. Grest, and M. P. Anderson, Phys. Rev. E **50**, 3361 (1994).
[10] A. Chakrabarti, Phys. Rev. Lett. **69**, 1548 (1992).
[11] B. J. Frisken, F. Ferri, and D. S. Cannell, Phys. Rev. Lett. **66**, 2754 (1991).
[12] B. J. Frisken and D. S. Cannell, Phys. Rev. Lett. **69**, 632 (1992).
[13] A. J. Bray, Phys. Rev. Lett. **62**, 2841 (1989).
[14] J. C. Lee, Phys. Rev. B **51**, 2661 (1995).
[15] P. C. Hohenberg and B. I. Halperin, Rev. Mod. Phys. **49**, 435 (1977); H. E. Stanley, *Introduction to Phase Transitions and Critical Phenomena* (Oxford University Press, New York, 1971); N. Goldenfeld, *Lectures on Phase Transitions and the Renormalization Group* (Addison-Wesley, Reading, MA, 1992).
[16] H. E. Stanley, in *Scaling Phenomena in Disordered Systems,* edited by R. Pynn and A. Skjeltorp (Plenum, New York, 1985).
[17] J. C. Lee, Phys. Rev. B **46**, R8648 (1992); Phys. Rev. Lett. **70**, 3599 (1993).
[18] J. C. Lee, Phys. Rev. E **52**, 4545 (1995).
[19] The idea was originally introduced by P. G. de Gennes, J. Phys. Chem. **88**, 6469 (1985), for binary liquids in a gel.